Thin Solid Films xxx (2015) xxx–xxx

Contents lists available at ScienceDirect

Thin Solid Films

journal homepage: www.elsevier.com/locate/tsf

Properties of $(NiO)_{1-x}(ZnO)_x$ thin films deposited by spray pyrolysis

L. Herissi [a,*], L. Hadjeris [a], M.S. Aida [b], J. Bougdira [c]

[a] LMSSEF, Oum El Bouaghi University, 04000, Algeria
[b] LCMI, Constantine 1 University, 25000, Algeria
[c] IJL UMR 7198, CNRS, Université de Lorraine, France

ARTICLE INFO

Article history:
Received 25 March 2015
Received in revised form 17 September 2015
Accepted 17 September 2015
Available online xxxx

Keywords:
Metal oxides
Thin films
Spray pyrolysis
Lattice constants
Electrical conductivity
Band gap

ABSTRACT

The main goal of the present work is the study of $(NiO)_{1-x}(ZnO)_x$ metal oxide thin films to determine their applicability in optoelectronic devices. For this purpose, well adherent films with $x = 0$, 0.25, 0.50, 0.75, and 1, were deposited by spray pyrolysis technique on glass substrates heated at 400 °C. Nickel chloride hexahydrate and zinc acetate dihydrate were used as precursors. Structural, electrical, optical and morphological properties of films have been studied. The obtained results indicate the formation of NiO and ZnO phases mixed in defined proportions for intermediate compositions and the lattice constant of NiO increases with the nominal fraction x of Zn. The dark electrical conductivity at room temperature varied between 10^{-9} and 10^{-5} $\Omega\ cm^{-1}$. A transmittance in the visible region situated between 50% and 80% was observed. The band-gap changes of the samples are situated between 3.21 eV and 3.74 eV.

1. Introduction

The deposition of thin films from solutions such as spray pyrolysis methods, catches the attention of researchers because these methods have several advantages namely: low-cost setup, ability to deposit large area layers, vacuum-less equipments, cost effectiveness, and flexibility over the conventional plasma film deposition methods [1]. This technique is used to deposit several metal oxide films including nickel oxide (NiO) and zinc oxide (ZnO) [1,2].

NiO has been under extensive investigations for decades due to its interesting electronic structure, strongly affected by Ni 3d electrons which are localized in space but spread out over a wide energy range because of strong Coulomb repulsion between them [3–5]. In spite of its partially filled 3d orbitals, NiO has a low electrical conductivity of p-type with a band-gap energy reported to be in the ultraviolet range (>3.5 eV) and has the NaCl crystal structure [5–7].

Recently, deposition of NiO thin films has attracted much attention due to their interesting electrical, magnetic and optical properties leading to a large number of technological applications such as: transparent conducting films, chemical sensors, magnetoresistance sensors, and electrodes in electrochromic smart windows [8–11].

ZnO films have good electro-optical properties suitable for optoelectronic applications. They are potential candidates for transparent front face electrodes and windows on solar cells and on flat panel displays [12]. Their high electromechanical coupling, hexagonal phase stability, and high piezoelectric constant make them useful in transducers [13]. Also, very sensitive ZnO gas detectors can be achieved by controlling the pore size in films microstructure [14].

Transition metals have many attracting properties and their alloys lead to new interesting features [15–17] which may improve optoelectronic properties. In this context, several authors [5,18–20] have prepared Zn:NiO and Ni:ZnO thin films by sol–gel method, pulsed laser deposition and spray pyrolysis, where their structural, optical, magnetic and electrical properties were characterized. The purpose of this study is to use the fact that the difference between NiO and ZnO structures may increase the porosity making their mixture useful for several applications such as gas sensor [21,22]. Also, NiO is a p-type material while ZnO is an n-type, thereafter, the conductivity type can be controlled by simply varying the nominal fraction x of Zn by depositing $(NiO)_{1-x}(ZnO)_x$ films. The conductivity evolves then from p-type with $x = 0$ towards n-type for $x = 1$. The aim of the present work is the preparation by spray pyrolysis technique of NiO, ZnO, and $(NiO)_{1-x}(ZnO)_x$ alloys thin films and the study of the influence of the x values on their structural, electrical, optical and morphological properties.

2. Experimental procedure

$(NiO)_{1-x}(ZnO)_x$ thin films were deposited by pneumatic spray pyrolysis technique from nickel chloride hexahydrate and zinc acetate dihydrate dissolved in doubly distilled water. Different values of the nominal fraction of Zn defined by $x = Zn / (Ni + Zn)$ were used (with $x = 0$, 0.25, 0.50, 0.75, and 1) and controlled through the variation of

* Corresponding author.
E-mail address: hlabidi12@gmail.com (L. Herissi).

http://dx.doi.org/10.1016/j.tsf.2015.09.034
0040-6090/

the solution concentration of precursor source of zinc and nickel separately. The experimental set up was previously described [23]. The layers have been deposited onto chemically cleaned microscopy glass substrates. Solution concentration, nozzle-substrate distance, substrate temperature, and spraying flow rate were kept constant during the whole deposition process at 0.05 mol/l, 30 cm, 400 °C and 9 ml/min, respectively. An estimated deposition time leading to a film thickness of about 0.3 μm was retained. The overall reaction process can be expressed as heat decomposition of nickel chloride hexahydrate or zinc acetate dihydrate to clusters of NiO or ZnO, respectively, in the presence of water and air oxygen [1,2,23].

Well adherent and transparent $(NiO)_{1-x}(ZnO)_x$ films were obtained. The film thickness was measured with a surface profilometer (Dektak 3st). The film structure was investigated by X-ray diffraction (XRD) using Philips X'Pert system and the Bragg–Bretano configuration (θ–2θ) operated at 40 kV, 40 mA with a filtered Cu:K_α radiation ($\lambda = 1.5418$ Å) at room temperature. The scanning angle 2θ is ranged from 20° to 80°. The electrical conductivity of $(NiO)_{1-x}(ZnO)_x$ thin films was measured using two-point probe, at room temperature, assuming homogenous conduction throughout the film depth. For this purpose two gold electrode stripes spaced by a gap of 1 cm were deposited on the film. The current–voltage characteristics were measured using a Keithley 616 digital electrometer and a stabilized direct current (DC) power supply. The film optical transmittance was recorded in the wavelength range from 300 to 1500 nm using an UV–Vis-NIR double beam spectrophotometer (SHIMADZU UV 3101 PC). Surface roughness of the films was observed by profilometry and atomic force microscopy (A100-AFM).

3. Results and discussion

3.1. Structural properties

The recorded XRD patterns of pure NiO ($x = 0$) and pure ZnO ($x = 1$) films, prepared with two substrate temperatures 400 and 450 °C, are reported in Fig. 1. As can be seen, the structure of ZnO thin film is not altered by the substrate temperature. On the contrary, the NiO film structure is degraded with increasing substrate temperature, according to the noticeable decrease in intensity of the peak located at 37.18° assigned to (111) plane. This decrease in the peak intensity with increasing substrate temperature of NiO films was observed by Kamal et al. It is related to the film thickness reduction caused by the reverse reaction which leads to the formation of amorphous nickel hydroxide at higher temperature [2]. According to this, we have fixed substrate temperature equal to 400 °C in the following.

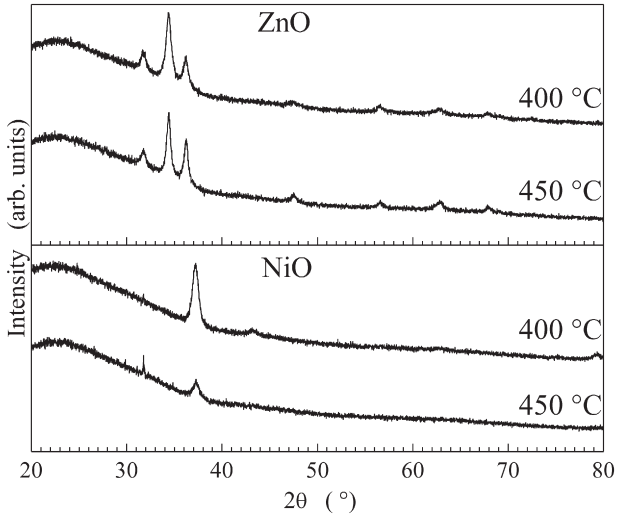

Fig. 1. XRD diffractograms of ZnO and NiO samples prepared at different substrate temperatures.

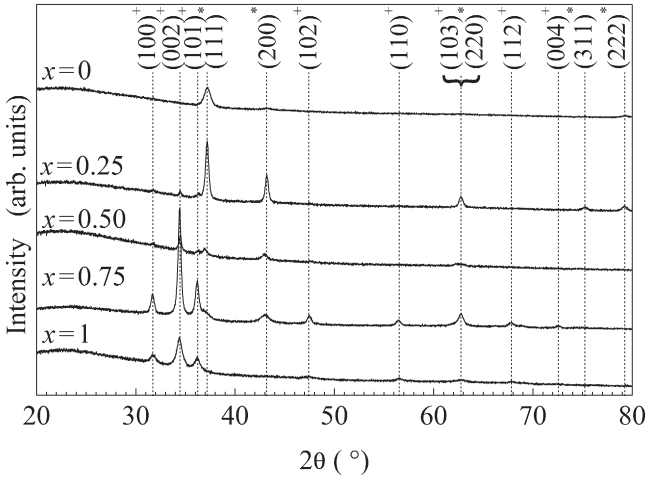

Fig. 2. XRD patterns of $(NiO)_{1-x}(ZnO)_x$ thin films as deposited on the amorphous substrates at 400 °C and 0.05 M for different x values. $(hkl)^*$ for NiO and $(hkl)^+$ for ZnO.

Fig. 2 shows the XRD pattern of $(NiO)_{1-x}(ZnO)_x$ thin films deposited by spray pyrolysis at 400 °C on glass substrates for different x values. The diffraction patterns indicate that the deposits are polycrystalline. At $x = 0$, only the NiO peaks of cubic phase are observed (ASTM 04-0835) and at $x = 1$, only the ZnO peaks of hexagonal phase (ASTM 36-1451) are present [24,25]. For intermediate compositions ($x = 0.25$, 0.50, and 0.75) the presence of both NiO and ZnO peaks indicates the formation of NiO and ZnO phases mixed in defined proportions, the relative intensity of the NiO peaks decreasing when the nominal fraction of Zn is increased. This observation is similar to the results obtained by other authors [26–28].

Fig. 3 shows the evolution of average grain size versus the ratio x in $(NiO)_{1-x}(ZnO)_x$ deposited at 400 °C and 0.05 M. We can note that the ZnO grains are larger than NiO ones. This behavior may be due to the difference in energy formation of ZnO and NiO. The formation enthalpy of ZnO ($\Delta H_f = -350.9$ kJ/mol) being less than that of NiO ($\Delta H_f = -239.9$ kJ/mol), the NiO formation is less favorable than the ZnO formation [29]. In addition to that, the ZnO and NiO crystallites size in mixture compound decreases when the nominal fraction of Zn increases in the precursor solution. This suggests that the growth of ZnO crystallites is easier in NiO matrix than in ZnO one. This is more consistent with the higher value of bulk modulus of NiO than that of ZnO. This parameter can be determined if we examine the relation

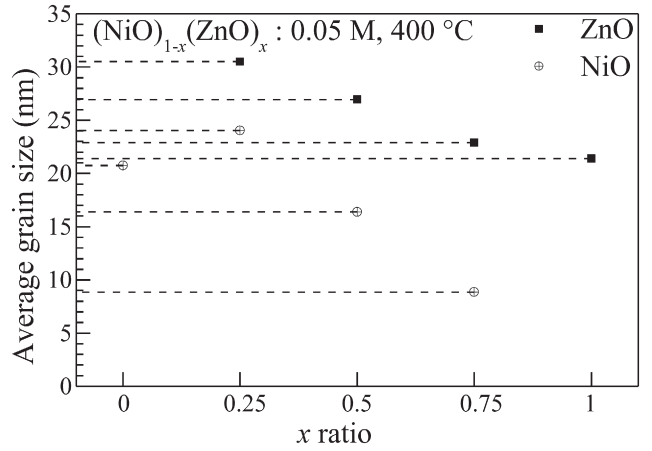

Fig. 3. Evolution of average grain size versus the ratio x in $(NiO)_{1-x}(ZnO)_x$ films deposited at 400 °C and 0.05 M.

Please cite this article as: L. Herissi, et al., Properties of $(NiO)_{1-x}(ZnO)_x$ thin films deposited by spray pyrolysis, Thin Solid Films (2015), http://dx.doi.org/10.1016/j.tsf.2015.09.034

(1), where the bulk modulus $B(T, P)$ depends both on the crystal structure and the elastic constants [9,12,19]:

$$B(T,P) \equiv -V_0\left(\frac{\partial P}{\partial V}\right)_T = \begin{cases} \dfrac{(c_{11}+c_{12})c_{33}-c_{13}^2}{c_{11}+c_{12}+2c_{33}-4c_{13}} & (hcp) \\ \dfrac{(c_{11}+2c_{12})}{3} & (fcc) \end{cases} \quad (1)$$

We can deduce the following bulk modulus values by using the elastic constants values ($c_{11} = 209.7$, $c_{12} = 121.1$, $c_{13} = 105.1$, $c_{33} = 210.9$, $c_{44} = 43$ GPa for ZnO [30], and $c_{11} = 450$, $c_{12} = 163$, and $c_{44} = 163$ GPa for NiO [31]):

$$\begin{cases} B_{ZnO} = 143 \ GPa \\ B_{NiO} = 258 \ GPa \end{cases} \quad (2)$$

One can see from Fig. 3 that the NiO grain size decreases when the nominal fraction of Zn increases. The effect of the compression being the volume reduction and because B_{NiO} is greater than B_{ZnO}, this means that it is more difficult to compress NiO than ZnO. This situation is more favorable to the growth of ZnO grains at the expense of NiO grains which are fragmented and have small-size.

The lattice constants (a and c) for both ZnO and NiO phases were calculated using Eq. (3) in the case of the hexagonal structure [32], and Eq. (4) for the cubic structure [33]:

$$d_{hkl} = \frac{a}{\sqrt{\frac{4}{3}\left(h^2+k^2+hk\right)+l^2\frac{a^2}{c^2}}} \quad (3)$$

$$d_{hkl} = \frac{a}{\sqrt{h^2+k^2+l^2}}. \quad (4)$$

The interplanar spacing "d_{hkl}" was determined by the Bragg's law (5) [34,35]:

$$2d_{hkl}\sin\theta_{hkl} = n\lambda \quad (5)$$

a_{ZnO} and c_{ZnO} values were deduced from (100) and (002) reflection peaks, respectively, while average a_{NiO} value was evaluated from (111) and (200) peaks using Eq. (6).

$$\begin{cases} a_{ZnO} = \dfrac{\lambda}{2.\sin\theta_{100}} \\ c_{ZnO} = \dfrac{\lambda}{\sin\theta_{002}} \\ a_{NiO} = \dfrac{\lambda\left(\sqrt{3}\sin\theta_{111}+2\sin\theta_{200}\right)}{8\sqrt{3}\sin\theta_{111}.\sin\theta_{200}}. \end{cases} \quad (6)$$

Fig. 4 shows the evolution of the lattice constants in $(NiO)_{1-x}(ZnO)_x$ films deposited at 400 °C and 0.05 M for different x values. The variation in a_{NiO} is situated between 4.18 Å and 4.22 Å ($\Delta a_{NiO} \approx 0.04$ Å) which is greater than the variation in a_{ZnO} and c_{ZnO}. This can be related to the difference of 0.05 Å in ionic radius of Ni and Zn ($r_{Ni}^{++} = 0.69$ Å and $r_{Zn}^{++} = 0.74$ Å). The larger variation of the lattice constants in NiO and the reduction of NiO crystallite size by comparison with ZnO is in good agreement with Fiévet et al. [36] who found that the lattice constant increased when the crystallites became small and also with Park et al. who found that the lattice constant a_{NiO} in $Ni_{1-x}Zn_xO$ increased linearly with the nominal fraction of Zn [5].

3.2. Electrical conductivity

The dark electrical conductivity of the $(NiO)_{1-x}(ZnO)_x$ films was measured using the conventional two-point probe. The current–voltage characteristics revealed a linear relation indicating an ohmicity of the electrical contacts. Fig. 5 shows the variation of the electrical conductivity (σ) of

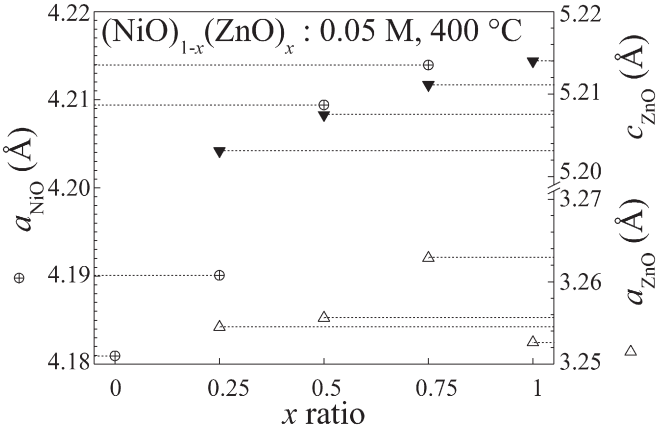

Fig. 4. Evolution of lattice constants versus the ratio x in $(NiO)_{1-x}(ZnO)_x$ films deposited at 400 °C and 0.05 M.

$(NiO)_{1-x}(ZnO)_x$ samples formed at different x values. As can be seen, the conductivity increases noticeably by three orders of decades (10^{-9}–10^{-5} Ω^{-1} cm^{-1}) with increasing the nominal fraction of Zn. On the one hand, we note that NiO is a p-type material and has a low conductivity [5–7,18,37], while ZnO is a n-type and has a high conductivity [23,38] due to the difference in hole and electron mobilities. Thereafter, the conductivity type of the deposited $(NiO)_{1-x}(ZnO)_x$ films can be controlled by simply varying the nominal fraction x. The conductivity evolves then from p-type with $x = 0$ towards n-type for $x = 1$.

On the other hand, as mentioned in §3.1, the presence of small crystallites, when $x \neq 1$, increases the grain boundaries which leads to a decrease in mobility and the degradation of the conductivity [39].

3.3. Optical and morphological properties

Spectral transmittance of $(NiO)_{1-x}(ZnO)_x$ films deposited by spray pyrolysis technique onto glass substrates at 400 °C and 0.05 M are shown in Fig. 6. The front edges of the curves represent the intrinsic absorption. The obtained films exhibit high transparency in the visible-NIR spectral region. The transmittance of ZnO ($x = 1$) is high while the transmittance for $x \neq 1$ is low between 400 and 600 nm due to the light scattering caused by the surface roughness [40]. This is consistent with AFM images, presented in Fig. 7, of the different samples of $(NiO)_{1-x}(ZnO)_x$ which show that the maximum depth ($\delta Z = 194$ nm) is minimum for $x = 1$ (ZnO) corresponding to the maximum of transmittance. For $x = 0$ (NiO) and $x = 0.75$, the values of Z are almost the same ($\delta Z = 280$ nm and $\delta Z = 303$ nm, respectively) so the

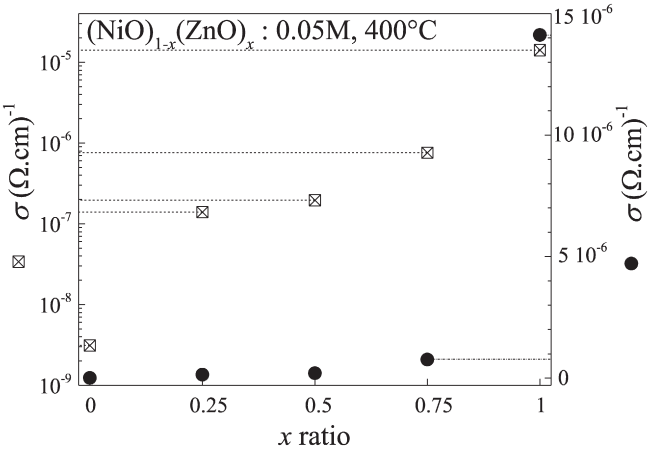

Fig. 5. Variation of electrical conductivity (linear and logarithmic scales) versus the ratio x in $(NiO)_{1-x}(ZnO)_x$ films deposited at 400 °C and 0.05 M.

Please cite this article as: L. Herissi, et al., Properties of $(NiO)_{1-x}(ZnO)_x$ thin films deposited by spray pyrolysis, Thin Solid Films (2015), http://dx.doi.org/10.1016/j.tsf.2015.09.034

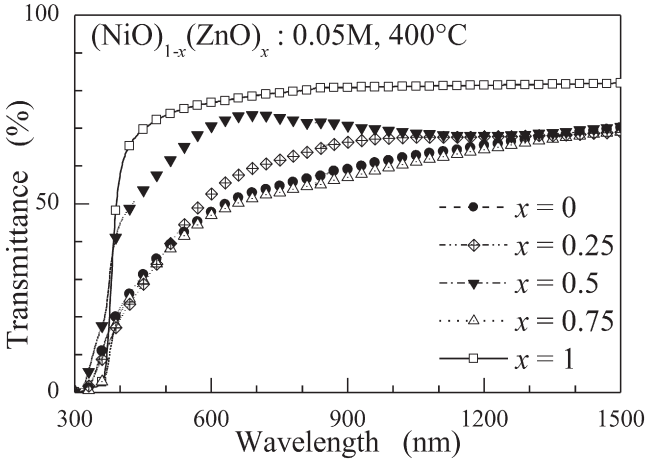

Fig. 6. Spectral variation of transmittance for $(NiO)_{1-x}(ZnO)_x$ films prepared at 400 °C and 0.05 M for different x values.

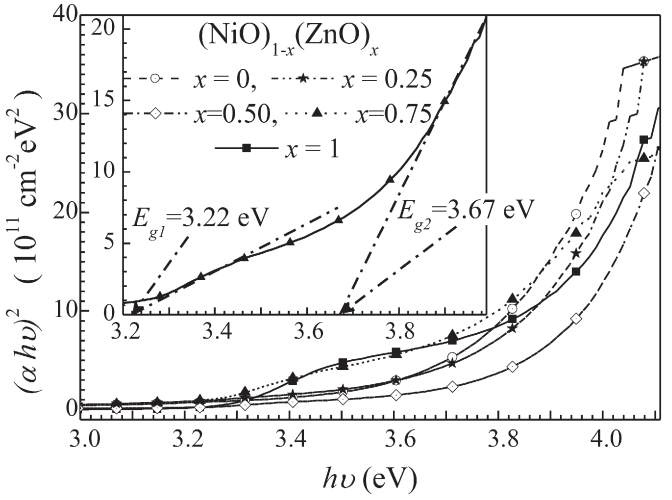

Fig. 8. The dependence of $(\alpha h\upsilon)^2$ on the incident photon energy $(h\upsilon)$ for $(NiO)_{1-x}(ZnO)_x$ films prepared at 400 °C and 0.05 M.

transmittance spectra are almost identical. For $x = 0.5$, the sample has a non-uniform thickness leading to a maximum depth ($\delta Z = 602$ nm) giving a higher transmittance and an XRD pattern with low intensity peaks (Fig. 2).

From these spectra we deduced the values of the optical energy gaps using Tauc's formula for direct band semiconductors [41]:

$$(\alpha h\upsilon)^2 = A(h\upsilon - E_g) \tag{7}$$

where A is a constant depending on the electron–hole mobility [28,42,43]. From $(\alpha h\upsilon)^2$ vs. $h\upsilon$ plot (Fig. 8.), E_g is obtained when $\alpha h\upsilon = 0$. a is the absorption coefficient deduced from the measured transmittance $T(\lambda)$ using Beer–Lambert law [23]:

$$\alpha = \frac{1}{d} \ln \frac{1}{T} \tag{8}$$

where d is the film thickness.

The optical band gap energies of $(NiO)_{1-x}(ZnO)_x$ samples formed at different x values are summarized in Table 1. The values found are located between 3.3 eV for ZnO ($x = 1$) and 3.7 eV for NiO ($x = 0$). For ($0 < x < 1$), there are two gap values, indicating the presence of two phases of ZnO and NiO as suggested by XRD analysis.

4. Conclusions

Well adherent $(NiO)_{1-x}(ZnO)_x$ films have been prepared by pneumatic spray pyrolysis technique on glass substrates from zinc acetate and nickel chloride solutions at 0.05 mol/l and 400 °C. The obtained results indicate that the films have surface roughness and their properties can be controlled through the nominal fraction of Zn. The XRD patterns indicate that the films are polycrystalline and show the presence of only one phase of NiO or ZnO when $x = 0$ or 1, respectively. For intermediate compositions ($x = 0.25$, 0.50 and 0.75), the $(NiO)_{1-x}(ZnO)_x$ films are composed of two phases mixed in defined proportions. The optical

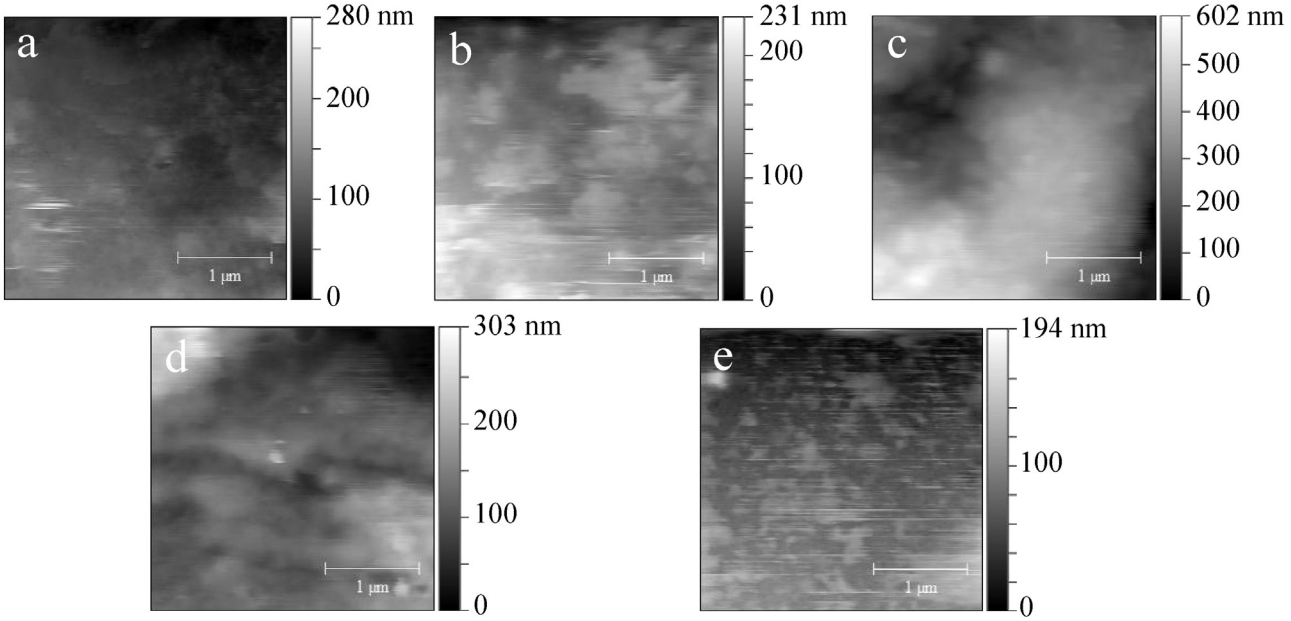

Fig. 7. AFM 2D images of $(NiO)_{1-x}(ZnO)_x$ films with different x values (a: $x = 0$, b: $x = 0.25$, c: $x = 0.50$, d: $x = 0.75$, and e: $x = 1$).

Please cite this article as: L. Herissi, et al., Properties of $(NiO)_{1-x}(ZnO)_x$ thin films deposited by spray pyrolysis, Thin Solid Films (2015), http://dx.doi.org/10.1016/j.tsf.2015.09.034

Table 1
Optical band gap energies of $(NiO)_{1-x}(ZnO)_x$ samples formed at different x values.

x	0.00	0.25	0.50	0.75	1.00
E_{g_1} (eV)	/	3.21	3.21	3.22	3.29
E_{g_2} (eV)	3.65	3.74	3.71	3.67	/

transmittance and electrical conductivity increase with the nominal fraction of Zn.

Acknowledgments

The authors would like to thank the members of LCAM-OEB laboratory for their help in achieving the AFM images.

References

[1] L. Hadjeris, L. Herissi, M. Benbouzid, N. Attaf, M.B. Assouar, T. Easwarakhanthan, M.S. Aida, J. Bougdira, A. Mahdjoub, Structural, optical and electrical characterization of transparent and semiconducting ZnO thin films grown by spray pyrolysis, Alger. J. Adv. Mater. 4 (2008) 9–12.
[2] H. Kamal, E.K. Elmaghraby, S.A. Ali, K. Abdel-Hady, Characterization of nickel oxide films deposited at different substrate temperatures using spray pyrolysis, J. Cryst. Growth 262 (2004) 424–434.
[3] W. Nolting, L. Haunert, G. Borstel, Temperature-dependent electronic structure and magnetic behavior of Mott insulators, Phys. Rev. B 46 (1992) 4426–4445.
[4] O. Bengone, M. Alouani, P.B. Ochl, J. Hugel, Implementation of the projector augmented-wave LDA + U method: application to the electronic structure of NiO, Phys. Rev. B 62 (2000) 16392–16401.
[5] Y.R. Park, K.J. Kim, Sol–gel preparation and optical characterization of NiO and $Ni_{1-x}Zn_xO$ thin films, J. Cryst. Growth 258 (2003) 380–384.
[6] H.-L. Chen, Y.-M. Lu, W.-S. Hwang, Characterization of sputtered NiO thin films, Surf. Coat. Technol. 198 (2005) 138–142.
[7] Y.-M. Lee, C.-H. Lai, Preparation and characterization of solid n-TiO2/p-NiO heterojunction electrodes for all-solid-state dye-sensitized solar cells, Solid State Electron. 53 (2009) 1116–1125.
[8] A. Surca, B. Orel, B. Pihlar, Characterization of redox states of Ni(La)-hydroxide films prepared via the sol–gel route by ex-situ IR spectroscopy, J. Solid State Electrochem. 2 (1998) 38–49.
[9] D.G. Hwang, S.S. Lee, C.M. Park, Effect of roughness slope on exchange biasing in NiO spin valves, Appl. Phys. Lett. 72 (1998) 2162–2164.
[10] K.S. Ahn, Y.C. Nah, Y.E. Sung, The effect of RF power on the electrochromic response time of sputter-deposited Ni oxide films, Jpn. J. Appl. Phys. 41 (2) (2002) L533–L535.
[11] C.M. Lampert, C.G. Granqvist, Large-area chromogenics: materials and devices for transmittance control, SPIE Ins. Adv. Technol., IS 4, 1990.
[12] S.A. Studenikin, N. Golego, M. Cocivera, Optical and electrical properties of undoped ZnO films grown by spray pyrolysis of zinc nitrate solution, J. Appl. Phys. 83 (4) (1998) 2104–2111.
[13] A. Elhichou, A. Bougrine, J.L. Bubendorff, J. Ebothe, M. Addou, M. Troyon, Structural, optical and cathodoluminescence characteristics of sprayed undoped and fluorine-doped ZnO thin films, Semicond. Sci. Technol. 17 (2002) 607–613.
[14] S.A. Studenikin, N. Golego, M. Cocivera, Fabrication of green and orange photoluminescent, undoped ZnO films using spray pyrolysis, J. Appl. Phys. 84 (4) (1998) 2287–2294.
[15] T. Dietl, H. Ohno, F. Matsukura, J. Clibert, D. Ferrand, Zener model description of ferromagnetism in zinc-blende magnetic semiconductors, Science 287 (2000) 1019–1022.
[16] X.M. Cheng, C.L. Chien, Magnetic properties of epitaxial Mn-doped ZnO thin films, J. Appl. Phys. 93 (2003) 7876–7878.
[17] K. Ueda, H. Tabata, T. Kawai, Magnetic and electric properties of transition-metal-doped ZnO films, Appl. Phys. Lett. 79 (7) (2001) 988–990.
[18] R. Noonuruk, W. Techitdheera, W. Pecharapa, Characterization and ozone-induced coloration of $Zn_xNi_{1-x}O$ thin films prepared by sol–gel method, Thin Solid Films 520 (2012) 2769–2775.
[19] S. Thota, L.M. Kukreja, J. Kumar, Ferromagnetic ordering in pulsed laser deposited $Zn_{1-x}Ni_xO$/ZnO bilayer thin films, Thin Solid Films 517 (2008) 750–754.
[20] V. Sharma, P. Kumar, J. Shrivastava, A. Solanki, V.R. Satsangi, S. Dass, R. Shrivastav, Synthesis and characterization of nanocrystalline $Zn_{1-x}M_xO$ (M = Ni, Cr) thin films for efficient photoelectrochemical splitting of water under UV irradiation, Int. J. Hydrog. Energy 36 (2011) 4280–4290.
[21] C.A. Canbay, A. Aydogdu, Microstructure, electrical and optical characterization of Zn0-NiO-SiO_2 nanocomposite synthesized by sol–gel technique, Turk. J. Sci. Technol. 4 (2) (2009) 121–126.
[22] C.H. Kwon, H.K. Hong, D.H. Yun, K. Lee, S.T. Kim, Y.H. Roh, B.H. Lee, Thick film zinc-oxide gas sensor for the control of lean air-to-fuel ratio in domestic combustion systems, Sensors Actuators B Chem. 25 (1995) 610–613.
[23] L. Hadjeris, L. Herissi, M.B. Assouar, T. Easwarakhanthan, J. Bougdira, N. Attaf, M.S. Aida, Transparent and conducting ZnO films grown by spray pyrolysis, Semicond. Sci. Technol. 24 (2009) 035006–6.
[24] L. Cattin, B.A. Reguig, A. Khelil, M. Morsli, K. Benchouk, J.C. Bernède, Properties of NiO thin films deposited by chemical spray pyrolysis using different precursor solutions, Appl. Surf. Sci. 254 (2008) 5814–5821.
[25] M. García-Hipólito, C.D. Hernández-Pérez, O. Alvarez-Fregoso, E. Martínez, J. Guzmán-Mendoza, C. Falcony, Characterization of europium doped zinc aluminate luminescent coatings synthesized by ultrasonic spray pyrolysis process, Opt. Mater. 22 (2003) 345–351.
[26] G. Santana, A.M. Acevedo, O. Vigil, F. Cruz, G.C. Puente, L. Vaillant, Structural and optical properties of $(ZnO)_x(CdO)_{1-x}$ thin films obtained by spray pyrolysis, Superf. Vacío 9 (1999) 300–302.
[27] W.T. Seeber, M.O. Abou-Helal, S. Barth, D. Beil, T. Höche, H.H. Afify, S.E. Demian, Transparent semiconducting ZnO:Al thin films prepared by spray pyrolysis, Mater. Sci. Semicond. Process. 2 (1999) 45–55.
[28] R. Romero, D. Leinen, E.A. Dalchiele, J.R. Ramos-Barrado, F. Martín, The effects of zinc acetate and zinc chloride precursors on the preferred crystalline orientation of ZnO and Al-doped ZnO thin films obtained by spray pyrolysis, Thin Solid Films 515 (2006) 1942–1949.
[29] J.-H. Lim, K.-K. Kim, D.-K. Hwang, H.-S. Kim, J.-Y. Oh, S.-J. Park, Formation and effect of thermal annealing for low-resistance Ni/Au ohmic contact to phosphorous-doped p-type ZnO, J. Electrochem. Soc. 152 (3) (2005) G179–G181.
[30] G.J. Hanna, S.T. Teklemichael, M.D. McCluskey, L. Bergman, J. Huso, Equations of state for ZnO and MgZnO by high pressure x-ray diffraction, J. Appl. Phys. 110 (2011) 073511–073515.
[31] M.D. Towler, N.L. Allan, N.M. Harrison, V.R. Saunders, W.C. Mackrodt, E. Aprà, Ab initio study of MnO and NiO, Phys. Rev. B 50 (8) (1994) 5041–5054.
[32] P. Prepelita, R. Medianu, B. Sbarcea, F. Garoi, M. Filipescu, The influence of using different substrates on the structural and optical characteristics of ZnO thin films, Appl. Surf. Sci. 256-6 (2009) 1807–1811.
[33] S. Kose, F. Atay, V. Bilgin, I. Akyuz, Some physical properties of copper oxide films: the effect of substrate temperature, Mater. Chem. Phys. 111 (2008) 351–358.
[34] H. Benzarouk, A. Drici, M. Mekhnache, A. Amara, M. Guerioune, J.C. Bernède, H. Bendjffal, Effect of different dopant elements (Al, Mg and Ni) on microstructural, optical and electrochemical properties of ZnO thin films deposited by spray pyrolysis (SP), Superlattices Microstruct. 52 (2012) 594–604.
[35] H.-L. Chen, Y.-M. Lu, W.-S. Hwang, Effect of film thickness on structural and electrical properties of sputter-deposited nickel oxide films, Mater. Trans. 46 (4) (2005) 872–879.
[36] F. Fiévet, P. Germi, F. de Bergevin, M. Figlarz, Lattice parameter, microstrains and non-stoichiometry in NiO. Comparison between mosaic microcrystals and quasi-perfect single microcrystals, J. Appl. Crystallogr. 12 (1979) 387–394.
[37] A.N. Banerjee, K.K. Chattopadhyay, Recent developments in the emerging field of crystalline p-type transparent conducting oxide thin films, Prog. Cryst. Growth Charact. Mater. 50 (2005) 52–105.
[38] S.Y. Myong, K.S. Lim, Improvement of electrical and optical properties of ZnO thin films prepared by MOCVD using UV light irradiation and in situ H2 post-treatment, Sol. Energy Mater. Sol. Cells 86 (1) (2005) 105–112.
[39] J.-H. Lee, B.-O. Park, Transparent conducting ZnO:Al, In and Sn thin films deposited by the sol–gel method, Thin Solid Films 426 (2003) 94–99.
[40] S.S. Shinde, P.S. Patil, R.S. Gaikwad, R.S. Mane, B.N. Pawar, K.Y. Rajpure, Influences in high quality zinc oxide films and their photoelectrochemical performance, J. Alloys Compd. 503 (2010) 416–421.
[41] J. Tauc, A. Menthe, States in the gap, J. Non-Cryst. Solids 8 (10) (1972) 569–585.
[42] G.G. Valle, P. Hammer, S.H. Pulcinelli, C.V. Santilli, Transparent and conductive ZnO: Al thin films prepared by sol–gel dip-coating, J. Eur. Ceram. Soc. 24 (6) (2004) 1009–1013.
[43] P.K. Nayak, J. Yang, J. Kim, S. Chung, J. Jeong, C. Lee, Y. Hong, Spin-coated Ga-doped ZnO transparent conducting thin films for organic light-emitting diodes, J. Phys. D: Appl. Phys. 42 (2009) 035102–035106.

Please cite this article as: L. Herissi, et al., Properties of $(NiO)_{1-x}(ZnO)_x$ thin films deposited by spray pyrolysis, Thin Solid Films (2015), http://dx.doi.org/10.1016/j.tsf.2015.09.034